

Estimation of Precipitation Area and Rain Intensity Based on the Microphysical Properties Retrieved from NOAA AVHRR Data

ITAMAR M. LENSKY AND DANIEL ROSENFELD

Institute of Earth Sciences, Hebrew University of Jerusalem, Jerusalem, Israel

(Manuscript received 4 December 1995, in final form 3 July 1996)

ABSTRACT

This paper investigates the feasibility of a quantitative estimation of precipitation from space, based on retrieval of microphysical properties of cloud tops using Advanced Very High Resolution Radiometer data. The effective radius r_e of cloud particles is calculated for highly reflective clouds in the visible wavelength, assuming that these are water clouds with infinite optical thickness at the 3.7- μm channel. A large effective radius indicates the presence of large droplets and/or ice in the clouds. The distinction between large droplets and ice is not necessary because the existence of either near the tops of thick clouds is conducive to the precipitation formation processes. In addition to the microphysical information, the fraction of rain cloud coverage and cloud spatial structure (convective and stratiform) were used for the rain estimation algorithm.

The satellite estimates were compared to radar data. Encouraging results were obtained for winter precipitation clouds in Israel with a wide range of cloud-top temperatures.

The method is not limited by temperature thresholds, resulting in estimates for rain intensity of clouds that do not necessarily contain large amounts of ice. Reasonable rain intensity estimates for clouds with relatively warm tops have not yet been obtained by other passive radiation methods, especially over land.

1. Introduction

Estimates of precipitation area and rain intensity from satellite data have been made for the past 25 years, with varying amounts of success. These methods can be divided into two main groups. The first uses visible (vis) reflected sunlight, and infrared (IR) radiation emitted from cloud tops; the second uses the emitted microwave (MW) radiation.

The vis-IR group consists of various methods with different degrees of complexity, ranging from methods using a single parameter, where the cloud area is the most common, such as the GPI-GOES (Geostationary Operational Environmental Satellite) precipitation index (Arkin and Meisner 1987)—to more complex techniques such as the CST (convective-stratiform technique) (Adler and Negri 1988). These methods assume that clouds with tops colder than a given threshold precipitate and the precipitation rate is a function of the cloud type. The split-window method (Inoue 1987) has remarkable success in classifying clouds, but does not give rain rates. However, it can be used to improve existing rain-rate estimation methods, by eliminating nonprecipitating clouds.

Rain-rate retrieval methods belonging to the passive MW group depend on the difference between the brightness temperature of raining clouds and the background (land or sea) in several wave bands. The cold background brightness temperature of water causes the MW rain estimates to perform well over water surfaces for most cloud types. However, the warm brightness temperature of land surfaces is similar to the rainfall signature in the MW. This leaves the ice signature as the main source of information for the MW rain estimate method over land. As a result, no current MW method is capable of reasonably accurate rain estimates for clouds with low ice content over land (Jones and Vonder Haar 1990).

While precipitation processes develop in practically all convective clouds with very cold tops, in clouds with warmer tops the precipitation processes are very sensitive to the microphysical structure of the cloud tops—that is, precipitation processes are more efficient when the droplets are larger or in the presence of ice. The main reason for the poor performance of vis-IR rain estimation methods for clouds with relatively warm tops is that they ignore the large variability of microphysical composition of clouds with temperatures warm enough to allow prolonged existence of supercooled water—that is, warmer than about 245 K.

The objective of this study is to show the feasibility of rain estimates based on the microphysical structure of cloud tops, retrieved from the reflected solar radiation

Corresponding author address: Dr. Daniel Rosenfeld, Institute of Earth Sciences, Hebrew University of Jerusalem, 91904 Jerusalem, Israel.
E-mail: daniel@vms.huji.ac.il

at 3.7 μm . This method is not limited by temperature thresholds, and thus it is inherently capable of providing rain estimates for clouds with relatively warm tops and little or no ice.

The rain estimates are based on the following steps:

- division of the scene into subareas (*windows*) large enough to contain a small convective cloud cluster (about 2000 km^2),
- exclusion of windows in which the potential rain clouds are obscured by overlaying clouds, and
- classification of the windows into rain types, based on the scale of inhomogeneity of the retrieved field of cloud-top particle size.

Windows with inhomogeneous fields were considered convective, and windows with relatively homogeneous fields were considered stratiform. Altogether four categories of rain types were considered, and each was treated separately.

2. The data

The data for this study were derived from the afternoon scan of the *NOAA-11* polar-orbiting satellite's Advanced Very High Resolution Radiometer (AVHRR) local area coverage over Israel and the east Mediterranean Sea. The AVHRR has a resolution of 1.1 km at nadir. The data were collected for February 1990 through March 1993, 98 windows from 33 different days altogether. All the data were used, without any meteorologically based selection.

The following channels of the radiometer were used.

- Channel 1 (0.65 μm) is usually utilized to estimate cloud optical thickness in that wave band (e.g., Arking and Childs 1985), which depends mainly on the vertically integrated amount of cloud condensates.
- Channel 3 (3.70 μm) is very sensitive to the cloud drop size distribution, to the thermodynamic phase, and to the particles shape (Arking and Childs 1985).
- Channel 4 (10.8 μm) provides the cloud-top blackbody brightness temperature, which approximates the cloud-top temperature, assuming that the atmosphere above the cloud is relatively dry.
- Channel 5 (12.0 μm), in conjunction with channel 4, provides information on cloud thickness and the vertically integrated water vapor in the atmosphere above the cloud top (Inoue 1987).

The AVHRR rain-rate retrieval algorithm was calibrated using a weather radar located at Ben-Gurion International Airport in Israel. The radar has a 5.4-cm wavelength and 1.6° beamwidth. The collocation between the satellite and radar data was done using the radar and satellite coordinates. The "window probability matching method" (Rosenfeld et al. 1994) was used for the radar rainfall intensity estimates. The standard error of the radar rain-rate measurements is under 15%.

3. Parameters for the rain estimates

The area of precipitating clouds is a major parameter used by most of the rain estimation algorithms. Rosenfeld and Gutman (1994) have shown that precipitation areas were well correlated with the area of cloud tops having an effective radius larger than 14 μm . Another widely used parameter is the classification of clouds into convective and stratiform (Adler and Negri 1988). The parameters used for the quantitative rain estimates in this study are described in this section.

a. The effective radius

The cloud-top microphysical properties are derived by comparing the radiance measured in channel 3 to the theoretically calculated radiance (Nakajima and King 1990). The effective radius r_e is defined as follows.

$$r_e \equiv \frac{\int_0^{\infty} r^3 n(r) dr}{\int_0^{\infty} r^2 n(r) dr}, \quad (1)$$

where $n(r)$ is the number size distribution as a function of particle radius r .

The algorithm for retrieving the effective radius of cloud droplets is that used by Rosenfeld and Gutman (1994). It consists of detection of optically thick cloud pixels in the satellite image and application of the model for retrieving the effective radius of cloud-top particles in these pixels.

The first step is the selection of pixels filled with clouds that are thick enough to be considered as potential precipitators. The selection was based on thresholding the channel 1 visible reflectance, the channel 4 brightness temperature, and the brightness temperature difference (BTD) of channels 4 and 5 as indications for optically thick clouds in the far IR (Inoue 1987). The following thresholds were selected for this study over Israel: visible reflectance higher than 40% indicates that the pixel is not partly filled with ground; temperatures were lower than a selected ground temperature of $T_g = 7^\circ\text{C}$; and BTD lower than 1°C indicated that we were not looking at optically thin clouds. These criteria are site specific and are based on the surface albedo and temperature. The parameters were empirically specified so that even slightly ambiguous pixels were rejected.

The second step assigns an effective radius to the selected pixel. The emitted 3.7- μm thermal radiation was eliminated, and then the effective radius was calculated based on the assumption that the cloud is composed exclusively of spherical water drops. In the case of ice, the absorption coefficient is nearly double that of water; in addition, ice crystals are usually much larger than cloud water droplets. Therefore, the 3.7- μm reflectance will be very low for clouds containing either ice crystals or very large water droplets near their tops.

The effect of either large water droplets or ice crystals is the same: initiation of the precipitation process. Therefore, the effective radius is used in this study as an index for the extent of precipitation formation processes in the clouds.

The pixels having 3.7- μm reflectance below 2% were considered to be cloud tops consisting mostly of ice particles. In this case no calculation of the effective radius was done. Note that large radii ($r_e > 25 \mu\text{m}$) typically coincide with very cold tops that can be assumed to be glaciated. For the rest of the pixels, the effective radius was calculated using the assumption that the cloud exclusively contained water droplets, while the interpretation of the results may involve any possible ice/water ratio.

b. Division of the viewed area into windows

The area within the range interval of 18–77 km from the radar was considered. This is the area for which radar rainfall estimates were available, using the window probability matching method (Rosenfeld et al. 1994) in Israel. This area was subdivided into several regions with nearly equal area of 2000 AVHRR pixels, equivalent to areas of 60 km \times 40 km, depending on the distance from the satellite nadir trajectory. This area is large enough to contain several whole rain clouds and was found to be meaningful in the following sense. Rosenfeld and Gagin (1989) have shown that when the area of a convective cloud cluster increases, the rain rate from this cloud cluster increases, up to a critical area of approximately 2000 km². Further increase of the cloud cluster area will not result in higher rain rate. The increase of rain intensity in windows containing a larger fraction of rainy area can be explained by the following observation: isolated clouds produce smaller rain intensities than clustered clouds reaching the same vertical growth (Rosenfeld and Gagin 1989). The main reason for this dependency is the fact that clouds in clusters protect each other from the detrimental effects of mixing with dry, midlevel ambient air. Other dynamic interactions between neighboring clouds may have effects that mutually enhance precipitation (Simpson et al. 1993). In addition, cloud clusters that grew beyond approximately 2000 km² probably already reached the maximum degree of mutual protection and enhancement, and the rain rate per unit area cannot be further increased.

By doing area comparisons we avoid one-to-one pixel matching problems such as

- needing exact navigation of radar coordinates to AVHRR coordinates;
 - having to match AVHRR cloud-top properties to cloud-base properties seen by the radar, for clouds under wind shear conditions where the cloud tops are not exactly located over their rain shaft; and the fact that because
- full radar volume scan takes about 5 min, different parts of the radar echo tops map are seen at different times. A 3-min difference between satellite and radar for a given pixel can be translated to a 10-km distance difference (with 50 m s⁻¹ wind speed at cloud-top altitude).
- All parameters in this paper, unless indicated otherwise, refer to a *window*.

c. Multilayered clouds detection algorithm

In a situation where there is more than one layer of clouds one on top of the other, their total visible optical depth may be large, whereas the satellite IR sensors detect only the top layer. In some cases there is no connection between the two layers, and while the lower layer precipitates, the upper layer is shallow and contains relatively small droplets. In cases like this, there is no correlation between the actual precipitation properties of the cloud and the indication of precipitation processes observed from the satellite.

The following algorithm was found useful in detecting areas of precipitating clouds under an incomplete nonprecipitating upper cloud layer.

- 1) Identify all the fully cloudy pixels in the window.
- 2) Find the average temperature of all pixels with $r_e > 14 \mu\text{m}$.
- 3) Divide all the pixels with $r_e > 14 \mu\text{m}$ into two subgroups, “warm pixels” and “cold pixels,” with respect to the average temperature.
- 4) Calculate the mean of r_e for the warm and cold subgroups.
- 5) Define the *layer index* as

$$\text{layer index} = \frac{\langle r_e(\text{warm}) \rangle}{\langle r_e(\text{cold}) \rangle}. \quad (2)$$

When all cloud tops in the window belong to clouds with the same vertical continuity, we expect $\langle r_e(\text{cold}) \rangle$ to be larger than $\langle r_e(\text{warm}) \rangle$. However, when a relatively thin layer overlies lower precipitating clouds, the radii of the upper-layer cloud droplets may be smaller than the lower layer. Therefore, a layer index larger than 1 is indicative of such a situation. In practice, the value of 1.02 was found to have the best discriminating power, compared to subjective classification.

d. “Convectivity” of clouds in the window

Cloud-top texture of stratiform clouds and large anvils is much more uniform than that of convective clouds with overshooting tops. This property is measured by the cloud radius parameter (CR_{sat}), which was constructed to be a quantitative index of the convectivity of clouds in the window; CR_{sat} is the average horizontal distance (km) for which the retrieved cloud-top droplet radii changes by a given percentage (15% in this study)

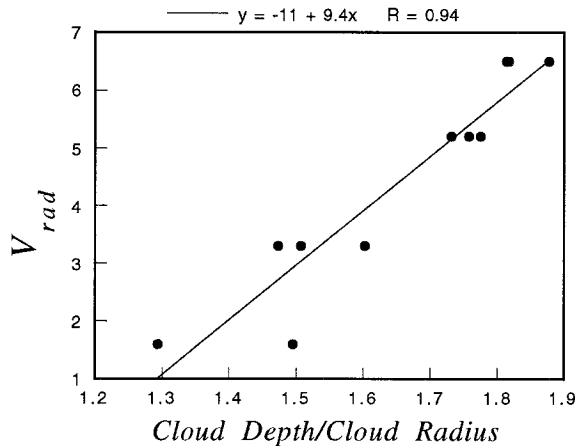


FIG. 1. Radar measurements of updraft velocity V_{rad} ($m\ s^{-1}$) vs radar-measured aspect ratio (cloud depth/cloud radius) for convective rain cells.

within the investigated window. A window with small CR_{sat} is interpreted as having convective clouds in it, while a window with large CR_{sat} is interpreted as containing stratiform clouds.

CR_{sat} was calculated in the following way.

- $CR_{sat}(i,j)$ was calculated for each cloudy pixel in the window by averaging the ranges in which the effective radii of neighboring pixels had changed by more than 15% in the four i,j directions, and
- $CR_{sat}(i,j)$ values were averaged over the window to give CR_{sat} .

Calculating CR_{sat} for different percentages results in different CR_{sat} values; however, this does not change its ability to be a good quantitative index for the convectivity of clouds in the window.

Rosenfeld (1986) studied various parameters of convective clouds over Israel and South Africa using radar data. Figure 1 was plotted using the radar data from his Fig. 7. In this figure the radar-inferred updraft velocity V_{rad} was plotted versus the aspect ratio of the precipitation cell as seen by the radar:

$$V_{rad} \propto \frac{\text{cloud depth}}{\text{cloud radius}} = \frac{D + 2}{(A/\pi)^{1/2}}, \quad (3)$$

where cloud depth was taken to be $D + 2$; D is the radar echo top height above freezing level in kilometers, and adding 2 km gives the cloud depth, assuming that freezing level is approximately 2 km higher than cloud base. The radar cloud radius was taken to be $(A/\pi)^{1/2}$, where A is the precipitation cell area (km^2).

Motivated by the high correlation between updraft velocity and precipitation cell aspect ratio, we aim to get an AVHRR updraft velocity estimate and to find a criterion to distinguish between convective and stratiform clouds. The first is achieved by using the cloud radius (CR_{sat}) parameter to estimate the mean horizontal dimension of clouds in the window. The mean vertical

TABLE 1. Relationship between satellite- and radar-observed precipitation areas for different cloud categories. Given are the correlation coefficient R , slope a , intercept b , and number of windows n for the different cloud categories.

Cloud type	Temperature	Multilayers	n	R	a	b
Convective	All	With	45	0.90	0.6	0.04
	All	Without	40	0.94	0.6	0.03
	$T > 245$ K	Without	26	0.92	0.6	0.03
	$T < 245$ K	Without	14	0.96	0.6	0.01
Stratiform	All	With	53	0.85	0.8	0.11
	All	Without	42	0.90	0.9	0.01
	$T > 245$ K	Without	21	0.51	0.5	0.14
	$T < 245$ K	Without	21	0.87	0.9	0.09

dimension ΔZ can be estimated by subtracting of mean height of cloud-top temperature in the window from the height of cloud-base temperature. We assumed that cloud-base temperature does not change significantly within the range interval of 18–77 km from the radar. Cloud-base temperature was taken to be the temperature of the warmest cloudy pixel plus $2^\circ C$ in that area, assuming that this pixel contains shallow undeveloped clouds of about 300-m height.

The AVHRR updraft velocity estimate V_{sat} is

$$V_{sat} \propto \frac{\Delta Z}{CR_{sat}}. \quad (4)$$

A discriminating criterion for convective or stratiform clouds was derived, assuming that the regression equation (5) for Fig. 1 represents convective clouds:

$$V_{rad} = -11 + 9.4 \left(\frac{\text{cloud depth}}{\text{cloud radius}} \right). \quad (5)$$

Clouds with zero vertical air velocity are definitely not convective. Therefore, the maximum possible aspect ratio for convective clouds is derived by setting $V_{rad} = 0$ in the regression equation (5) of Fig. 1:

$$\text{cloud radius} = \frac{\text{cloud depth}}{1.2}, \quad (6)$$

and rewriting (6) with AVHRR-derived parameters results in

$$CR_{max} = \frac{\Delta Z}{1.2}, \quad (7)$$

where CR_{max} is the maximum cloud radius (CR_{sat}) for a given cloud depth, which can still be called ‘‘convective.’’ Windows with CR_{sat} larger than CR_{max} will be regarded as windows with stratiform clouds.

Table 1 shows the number of windows in each class, indicating multilayered clouds windows, cloud type, and temperature.

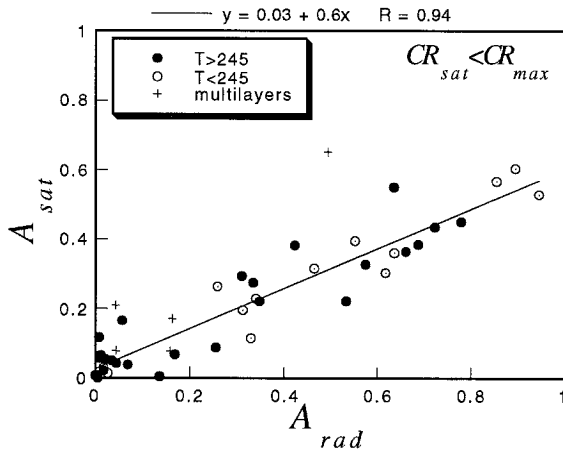


FIG. 2. Fraction of precipitating area, defined by the area with $r_e > 14 \mu\text{m}$ (A_{sat}), as a function of the fraction of precipitating area detected by the radar (A_{rad}) for convective clouds ($CR_{\text{sat}} < CR_{\text{max}}$). Windows with multilayered clouds are marked with crosses, windows with cloud-top temperatures higher than 245 K are marked with solid circles, and windows with cloud-top temperatures lower than 245 K are marked with hollow circles.

4. Quantitative estimates

a. Precipitation area

Each window was assigned the following parameters: cloud type (convective/stratiform); layer index; fraction of the window covered with radar precipitation echoes; and fraction of window covered with effective radii greater than $14 \mu\text{m}$, which was found best correlated with radar precipitation echoes (Rosenfeld and Gutman 1994).

Figure 2 displays the relationship between the fraction of precipitating area, defined by the area with $r_e > 14 \mu\text{m}$ (A_{sat}), and the fraction of precipitating area detected by the radar (A_{rad}) for windows containing convective clouds ($CR_{\text{sat}} < CR_{\text{max}}$). The solid circles stand for windows with cloud-top temperatures higher than 245 K, and the hollow circles stand for windows with cloud-top temperatures lower than 245 K. There are 45 windows in this figure; 5 of them (marked by a cross) contain multilayered clouds. A regression line for the windows with no multilayered clouds is shown. The regression lines of the two temperature subgroups were almost identical (see Table 1).

The relationship between A_{sat} and A_{rad} for stratiform clouds is given in Fig. 3. There are 53 windows in this figure; 11 of them (marked by a cross) contain multilayered clouds. We can see that the warmer clouds (solid circles) do not cover more than half of the window area ($A_{\text{sat}} < 0.5$), while the colder clouds (hollow circles) may expand up to the full window area.

The correlation coefficient is higher when the multilayered windows are not included, although the total number of windows decreases. Table 1 shows the regression coefficients and number of windows for all the data. The slope of the regression line is larger for win-

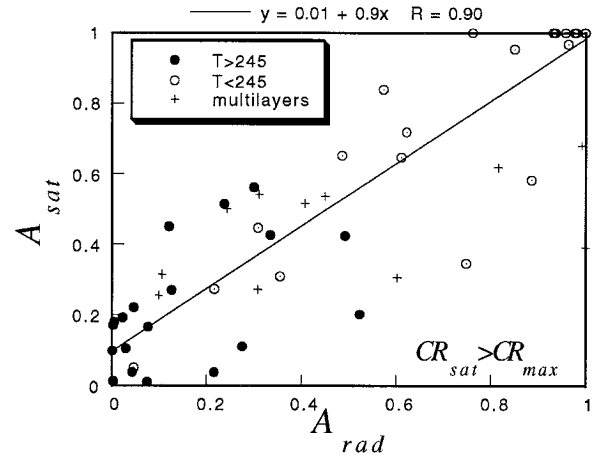


FIG. 3. As in Fig. 2 except for stratiform clouds ($CR_{\text{sat}} > CR_{\text{max}}$).

dows containing stratiform clouds (0.9) than for windows containing convective clouds (0.6)—that is, A_{sat} for given echo area is larger for stratiform clouds. This means that a larger area of the cloud tops contains particles with $r_e > 14 \mu\text{m}$ for the same precipitation area (A_{rad}). This may be due to the longer time that is available for the growth and glaciation of cloud particles in stratiform clouds. Liou (1992) suggested a bimodal size distribution for the description of data collected from clouds such as nimbostratus and cumulus congestus. He suggested a linear combination of two gamma distribution functions with modes 4 and $7 \mu\text{m}$ for cumulus congestus and 4 and $10 \mu\text{m}$ for nimbostratus. The larger mode radii for the nimbostratus clouds support the finding that the slope of the regression line of stratiform clouds is larger than that of convective clouds.

b. Rainfall

Different rain formation processes are dominant in convective and stratiform clouds, which results in large differences between the cloud-top properties and the rain intensities. This requires different approaches to rain-rate estimation for the different rain types. Therefore, the dataset was divided into subgroups. Rain-rate estimates for convective clouds are based on the relationships between factors such as area, depth, duration, and updraft velocity, as quantitatively shown by Rosenfeld and Gagin (1989). A simple water vapor flux model was used for the rain-rate estimates of the stratiform clouds. As a first guess, the fraction of precipitating area A_{sat} was plotted as a function of R in each window, where R (mm h^{-1}) is the average rain rate over the raining area (see Fig. 4). The large variability in the rain intensities, as evident in Fig. 4, precludes the possibility of using area–rainfall relationships, as used in the GPI (Arkin and Meisner 1987) or in the area–time integral (ATI) (Donneaud et al. 1984; Atlas et al. 1990; Rosenfeld et al. 1990). In addition to the area, the re-

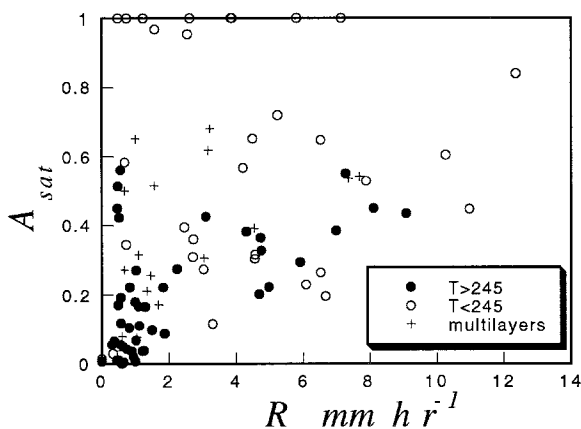


FIG. 4. Fraction of precipitating area, defined by the area with $r_c > 14 \mu\text{m}$ (A_{sat}), as function of radar rain rate R in each window. Windows with multilayered clouds are marked with crosses, windows with cloud-top temperatures higher than 245 K are marked with solid circles, and windows with cloud-top temperatures lower than 245 K are marked with hollow circles.

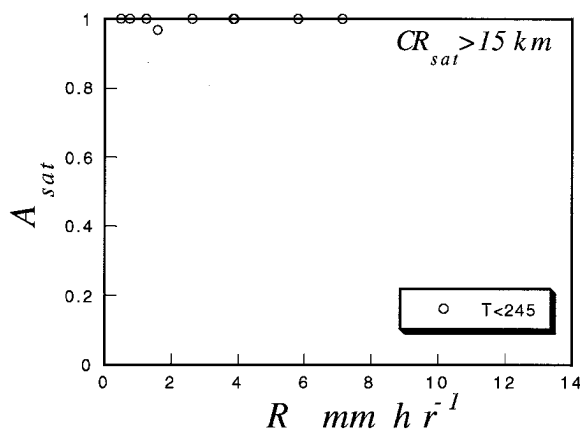


FIG. 6. Same as Fig. 4 but only for windows in which $CR_{\text{sat}} > 15 \text{ km}$, which are interpreted as stratiform rain windows.

trieved cloud-top properties must be used to obtain additional information about the rain intensities.

Three different rain types are noted in Fig. 4.

- 1) The points on the line $A_{\text{sat}} \approx 1$ are due to fully clouded windows, with large anvils or extensive stratiform clouds.
- 2) The main group along the diagonal has the characteristic features of convective clouds: the rain rate R increases with increasing cloud area.
- 3) Finally, there are clouds with small rain rates ($0 < R < 2 \text{ mm h}^{-1}$) with variable fractions of the rainy area (A_{sat}).

To check whether these three subgroups are indeed related to the “convectiveness,” we used the cloud radius parameter (CR_{sat}). A histogram of CR_{sat} for all windows without multilayered clouds is plotted in Fig. 5. Note

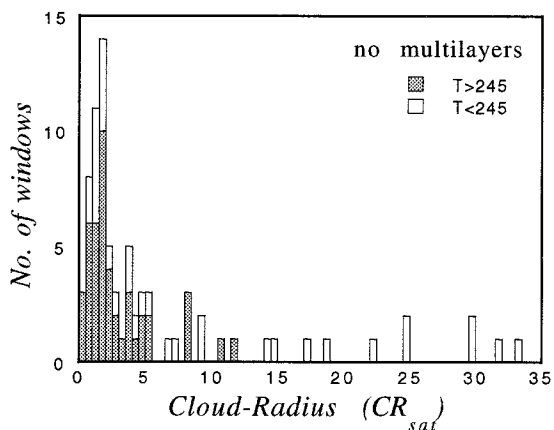


FIG. 5. Frequency distribution of the cloud radius parameter (CR_{sat}), the average distance (km) over which the retrieved effective radii of cloud droplets near their tops change by 15%.

that in this figure the bigger CR_{sat} ($> 14 \text{ km}$) belong to the colder clouds ($T < 245 \text{ K}$); the warmer clouds ($T > 245 \text{ K}$) have smaller CR_{sat} ($< 12 \text{ km}$); and the colder clouds’ cloud radii are distributed in an almost even way.

The partition between the three rain types was expected to be manifest also in the values of CR_{sat} . The windows with $CR_{\text{sat}} > 15 \text{ km}$ were defined as extensive stratiform clouds. Indeed, as can be seen in Fig. 6, all of these windows had nearly 100% rain cloud coverage. The windows with $CR_{\text{sat}} < 3.5 \text{ km}$ show convective behavior (see Fig. 7), by virtue of having higher rain intensities for larger rain areas (Rosenfeld and Gagin 1989). Figure 8 shows the remaining intermediate values of CR_{sat} . They are interpreted as stratiform and weak convective clouds, and are named here as precipitating “intermediate” (between convective and stratiform) clouds. These three groups correspond to the three rain types noted in Fig. 4.

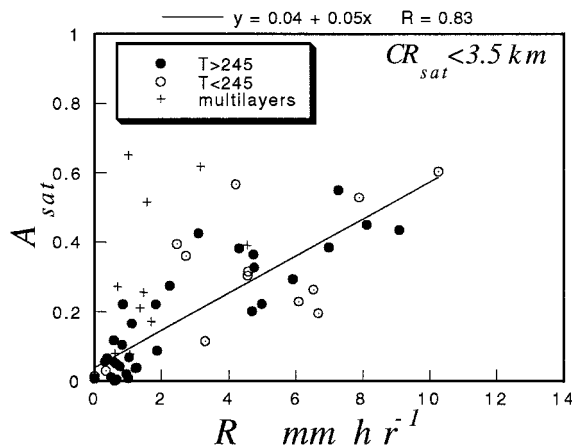


FIG. 7. Same as Fig. 4 but only for windows in which $CR_{\text{sat}} < 3.5 \text{ km}$, which are interpreted as convective rain windows.

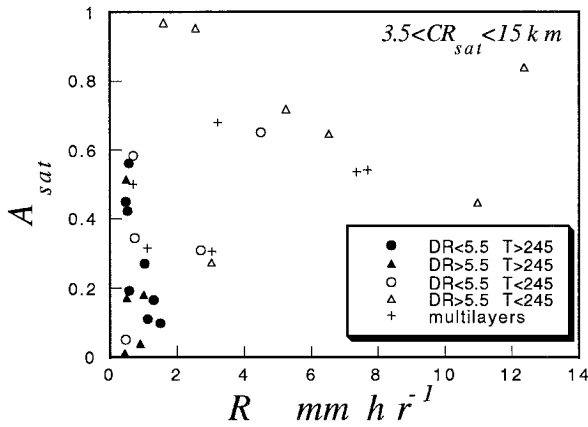


FIG. 8. Same as Fig. 4 but only for windows in which $3.5 < CR_{sat} < 15$ km, which are interpreted as transitional between weak convective and stratiform rain windows. Triangles refer to $5.5 < CR_{sat} < 15$ km and circles to $3.5 < CR_{sat} < 5.5$ km.

c. Convective clouds

To check the validity of $CR_{sat} = 3.5$ km as a separator between convective and other cloud types, all windows with $CR_{sat} < CR_{max}$ were plotted in Fig. 9 in the same manner as in Fig. 7. The fact that most points are common to both Figs. 7 and 9 can be considered to be a verification of our findings by an independent approach.

It has been shown in Figs. 7 and 9 that

$$R \propto A_{sat} \tag{8}$$

We wish to estimate the averaged rain rate over the full window area ($\langle R \rangle$). This parameter is connected to R via

$$\langle R_{sat} \rangle = RA_{sat} \tag{9}$$

Substituting (8) in (9) gives

$$\langle R_{sat} \rangle \propto (A_{sat})^2 \tag{10}$$

Based on (10), Fig. 10 presents the high correlation between $\langle R_{rad} \rangle$ and $(A_{sat})^2$. The correlation coefficient reached 0.87 for the convective clouds rain-rate estimation. The nearly even mix between the warmer and the colder cloud windows suggests that for convective clouds there is no fundamental difference between warm and cold clouds with respect to the 245-K threshold. The common assumption, used by most vis-IR methods, that precipitation exists only in clouds colder than a specified threshold can be avoided by using the method suggested here.

d. Precipitating intermediate clouds

This class of clouds is the intermediate group between well-defined convective clouds and extensive stratiform clouds. For this class of clouds we used the simple water vapor flux model

$$R_{sat} = (W_{base} - W_{top})V_{sat}E(r_e) \tag{11}$$

$$\langle R_{sat} \rangle = R_{sat}A_{sat} \tag{12}$$

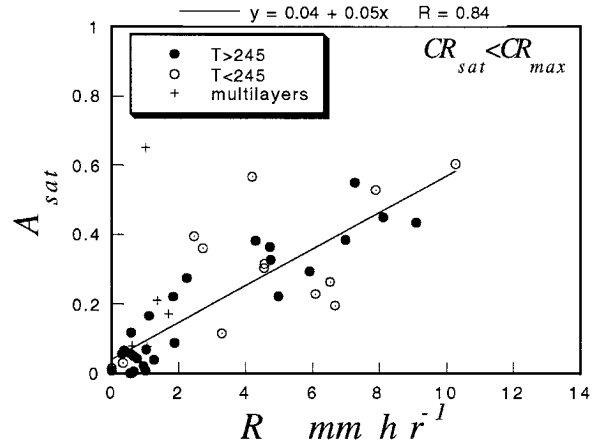


FIG. 9. Same as Fig. 4 but only for windows in which $CR_{sat} < CR_{max}$, which are interpreted as convective rain windows.

where $\langle R_{sat} \rangle$ is the satellite estimate for average rain rate over the window, W_{base} is the water vapor mixing ratio at the cloud base, W_{top} is the water vapor mixing ratio at the cloud top, and $E(r_e)$ is the conversion efficiency of cloud condensates to rainfall. The water vapor mixing ratio was calculated from

$$W_x = 0.622 \frac{e_s(T_x)}{P_x - e_s(T_x)} \tag{13}$$

where x stands for cloud base or cloud top, T_x (K) is the temperature, P_x (mb) is the air pressure, and $e_s(T)$ (mb) is the water vapor partial pressure.

Here $e_s(T_x)$ can be fitted within 0.1% over the temperature range of $-30^\circ\text{C} < T < 35^\circ\text{C}$ by the empirical formula (Rogers and Yau 1991)

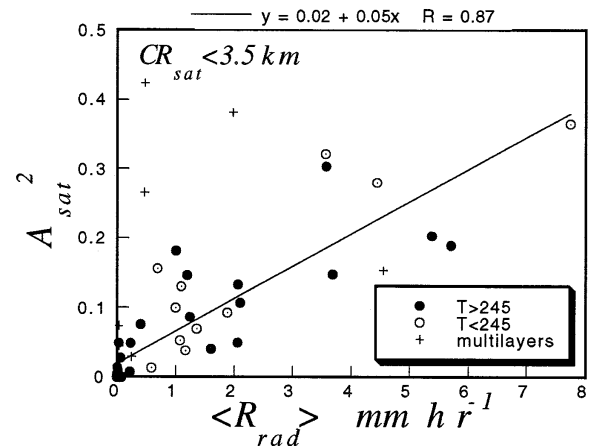


FIG. 10. The relation between the averaged rain rate over the whole window $\langle R_{rad} \rangle$ and the square of the rainfall fractional coverage of the window $(A_{sat})^2$ for convective clouds with $CR_{sat} < 3.5$ km. Windows with multilayered clouds are marked with crosses, windows with cloud-top temperatures higher than 245 K are marked with solid circles, and windows with cloud-top temperatures lower than 245 K are marked with hollow circles.

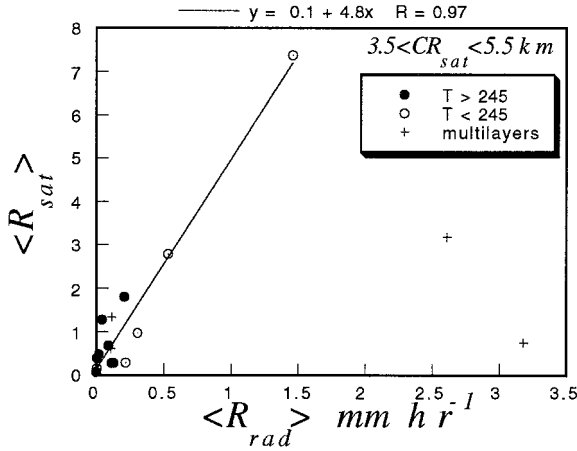


FIG. 11. The relation between the averaged rain rate over the whole window $\langle R_{rad} \rangle$ and the satellite estimation $\langle R_{sat} \rangle$ for windows in which $3.5 < CR_{sat} < 5.5$ km (weak convective to stratiform clouds). Windows with multilayered clouds are marked with crosses, windows with cloud-top temperatures higher than 245 K are marked with solid circles, and windows with cloud-top temperatures lower than 245 K are marked with hollow circles.

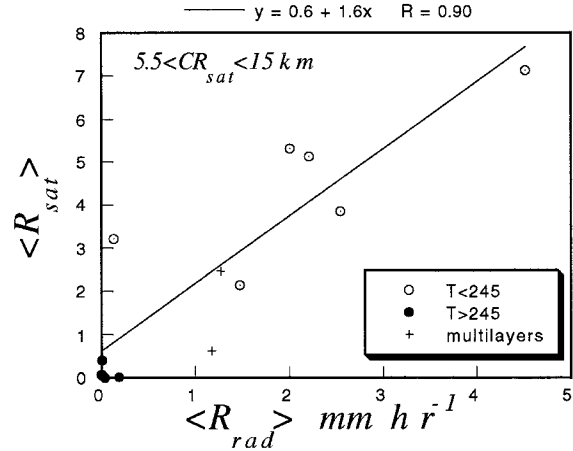


FIG. 12. The same as Fig. 11 but for windows in which $5.5 < CR_{sat} < 15$ km (stratiform clouds).

$$e_s(T) = 6.112 \exp\left(\frac{17.67T}{T + 243.5}\right), \quad (14)$$

where e_s is in millibars and T is in degrees Celsius.

The parameterization of the conversion efficiency of cloud water to rain $E(r_e)$ was done in the belief that the effective radius at cloud top is an indicator of the efficiency of coalescence processes or the amount of ice in the cloud. The range of values of the effective radius of precipitating clouds is $14 < r_e < 30 \mu\text{m}$, where $14 \mu\text{m}$ is the threshold value for precipitating clouds and $30 \mu\text{m}$ is the “saturation” value of the calculation of the effective radius. The parameterization took the form of

$$E(r_e) = \frac{\sum_{N_{14}} \left(\frac{r_e - 14}{30 - 14}\right)^{0.3}}{N_{14}}. \quad (15)$$

The summation is over all pixels with $r_e > 14 \mu\text{m}$ in a window (N_{14}). The correlation coefficient in Figs. 11 and 12 was slightly higher when using a power of 0.3 than other powers in the (0,1) interval.

In (11), V_{sat} for the intermediate group was constructed to be a linear function of the cloud aspect ratio, in the same way that V_{sat} for convective clouds was constructed, but with different coefficients. The calculation of the coefficients was based on the following assumptions.

- Clouds with zero aspect ratio have zero updraft velocity.
- The lower end of convective clouds should match the upper end of the intermediate cloud group (aspect ratio 1.33; $V_{sat} = 1.5$ in Fig. 1). The following equation was obtained: $V_{sat} = 1.1\Delta Z/CR_{sat}$.

The intermediate cloud group was further divided into two subgroups: one with $3.5 < CR_{sat} < 5.5$ km, which was found to contain mostly small anvil growing from convective activity, and the second with $5.5 < CR_{sat} < 15$ km, which was found to contain larger stratiform clouds. Figures 11 and 12 show the relations between the satellite estimation for the rain rate $\langle R_{sat} \rangle$ and the radar estimation $\langle R_{rad} \rangle$ for the two groups.

Note the difference between the slopes of the regression curves in Figs. 11 and 12. The rain rates in Fig. 11 are overestimated compared to Fig. 12 for the same $\langle R_{rad} \rangle$. This relative overestimation of $\langle R_{sat} \rangle$ can be due to V_{sat} or $E(r_e)$. Both parameters are likely to be higher for mature deep convective clouds than for mostly stratiform clouds. The small sample size is insufficient to determine to what extent this is a representative situation.

e. Extensive stratiform clouds

Since the extensive stratiform clouds typically fill the whole window, no correlation can exist between the rain area and the rain rate (see Fig. 6). Rain-rate values depend on cloud depth and cloud horizontal extent. Neither could be retrieved from a fully clouded window.

For these situations the best that can be done is to assign the average radar rain rates to these windows. The average rain rate R for the extensive stratiform clouds was 3 mm h^{-1} , with a standard deviation of 2.3 mm h^{-1} , in agreement with the well-established GPI method rain rate (Arkin and Meisner 1987).

Most of the extensive stratiform clouds have very cold tops; therefore, no additional information is expected to be gained by the effective radius derived from channel 3, and the method then degenerates to the GPI.

5. Summary and conclusions

A new algorithm is suggested for estimating rain area and rain rates from multispectral data (National Oceanic

and Atmospheric Administration AVHRR and GOES today). The main steps of the algorithm are as follows.

- 1) Detect fully clouded pixels.
- 2) Assign an effective radius of cloud-top particles to these pixels.
- 3) Divide the area into windows of 2000 AVHRR pixels each.
- 4) Assign each window one of the four convective to stratiform cloud types by the cloud radius parameter.
- 5) Assign rain area and rain rate to each of the cloud types.

Most methods assume that all clouds with top temperatures lower than a given threshold precipitate (excluding cirrus clouds). These methods assume implicitly that the other clouds do not precipitate. This study shows that it is possible to identify precipitating clouds with relatively warm tops by multispectral analysis and that clouds with top temperatures higher than 245 K show large variability of rain rate. The temperature, therefore, is not useful for retrieving the rain rate from such clouds. Once the precipitating clouds were delineated, they were divided into different types and assigned rain rates, irrespective of the cloud-top temperatures.

In addition to the microphysical information, it was found that the organization of convective clouds is very useful for the quantitative rain estimates. It was demonstrated that the area of convective cloud clusters that are smaller than the window (about 2000 km²) is correlated with the rain rate. Therefore, for convective clouds the rain rate in the window $\langle R \rangle$ is proportional to the square of the fractional coverage by precipitation. It is likely, therefore, that the use of the area of precipitating clouds (A_{sat}) has the potential to improve the rain-rate estimates of the existing methods.

In addition to the visible and IR wave bands, microwave frequencies are widely used for rain estimation from satellites. The existing microwave methods are, for the most part, successful in monitoring global precipitation (Grody 1991). However, rain from clouds without large ice particles is not easily detected over land due to the high surface emissivity. In addition, microwave sensors do not presently allow resolution of the convective cloud scale, thus introducing bias errors. Nearly one-third of the rainfall is precipitated from such clouds in Israel (Rosenfeld and Gutman 1994).

Acknowledgments. We wish to thank Dr. G. Gutman for the AVHRR data, Dr. M. King and Dr. T. Nakajima for the use of their radiation transfer model, Mrs. Tsipora Weinberg for the model adaptation and calculations of the effective radius, and to E.M.S. for the radar data. The remarks of a referee greatly improved the clarity of the paper, and we are grateful to him. This research was supported by a grant from the United States–Israel Binational Science Foundation in Jerusalem, Israel.

APPENDIX

List of Symbols

A_{rad}	cloud area divided by window area measured by the radar
A_{sat}	cloud area divided by window area measured by the satellite
CR_{max}	maximal cloud radius for convective clouds
CR_{rad}	radar-retrieved cloud radius
CR_{sat}	satellite-retrieved cloud radius
ΔZ	satellite-retrieved cloud depth
$E(r_e)$	conversion efficiency of cloud water to rain
N_{14}	number of pixels with $r_e > 14 \mu\text{m}$ in the window
R	averaged rain rate (mm h ⁻¹) over the raining area
r_e	effective radius of cloud-top particles
$\langle R_{\text{sat}} \rangle$	averaged rain rate over the window measured by the satellite
$\langle R_{\text{rad}} \rangle$	averaged rain rate over the window measured by the radar
V_{rad}	updraft velocity measured by the radar
V_{sat}	updraft velocity measured by the satellite

REFERENCES

- Adler, R. F., and A. J. Negri, 1988: A satellite infrared technique to estimate tropical convective and stratiform rainfall. *J. Appl. Meteor.*, **27**, 30–51.
- Arkin, P. A., and B. N. Meisner, 1987: The relationship between large-scale convective rainfall and cold cloud over the Western Hemisphere during 1982–84. *Mon. Wea. Rev.*, **115**, 51–74.
- Arking, A., and J. D. Childs, 1985: Retrieval of cloud cover parameters from multispectral satellite images. *J. Climate Appl. Meteor.*, **24**, 322–333.
- Atlas, D., D. Rosenfeld, and D. Short, 1990: The estimate of convective rainfall by area integrals. Part I: The theoretical and empirical basis. *J. Geophys. Res.*, **95**, 2153–2160.
- Donneaud, A. A., S. I. Niskov, D. L. Priegnitz, and P. L. Smith, 1984: The area–time integral as an indicator for convective rain volumes. *J. Appl. Meteor.*, **23**, 555–561.
- Grody, N. C., 1991: Classification of snow and precipitation using the Special Sensor Microwave Imager. *J. Geophys. Res.*, **96**, 7423–7435.
- Inoue, T., 1987: An instantaneous delineation of convective rainfall areas using split window data of NOAA-7 AVHRR. *J. Meteor. Soc. Japan*, **65**, 469–481.
- Jones, A. S., and T. H. Vonder Haar, 1990: Passive microwave remote sensing of cloud liquid water over land. *J. Geophys. Res.*, **95**, 16 673–16 683.
- Liou, K. N., 1992: *Radiation and Cloud Processes in the Atmosphere*. Oxford University Press, 487 pp.
- Nakajima, T., and M. D. King, 1990: Determination of the optical thickness and effective particle radius of clouds from reflected solar radiation measurements. Part I: Theory. *J. Atmos. Sci.*, **47**, 1878–1893.
- Rogers, R. R., and M. K. Yau, 1991: *A Short Course in Cloud Physics*. 3d ed. Pergamon Press, 293 pp.
- Rosenfeld, D., 1986: The influence of instability on the updraft velocity and on the precipitation properties of convective cumuli. Preprints, *23d Int. Conf. on Radar Meteorology*, Snowmass, CO, Amer. Meteor. Soc., JP321–JP324.
- , and A. Gagim, 1989: Factors governing the total rainfall yield of continental convective clouds. *J. Appl. Meteor.*, **28**, 1015–1030.
- , and G. Gutman, 1994: Retrieving microphysical properties of cloud tops by multispectral analysis of AVHRR data. *J. Atmos. Res.*, **34**, 259–283.
- , D. Atlas, and D. A. Short, 1990: The estimation of rainfall by area integrals. Part 2. The Height–Area Rain Threshold (HART) method. *J. Geophys. Res.*, **95**, 2161–2176.
- , D. B. Wolff, and E. Amitai, 1994: The window probability matching method for rainfall measurements with radar. *J. Appl. Meteor.*, **33**, 683–693.
- Simpson, J., T. D. Keenan, B. Ferrier, R. H. Simpson, and G. Holland, 1993: Cumulus mergers in the Maritime Continent region. *Meteor. Atmos. Phys.*, **51**, 73–99.